Research Article | Vol. 24, No. 25 | 12 Dec 2016 | OPTICS EXPRESS 28659

Optics EXPRESS

Diffraction-free pulsed optical beams via space-time correlations

H. Esat Kondakci and Ayman F. Abouraddy*

CREOL, The College of Optics & Photonics, University of Central Florida, Orlando, Florida 32816, USA
*raddy@creol.ucf.edu

Abstract: Diffraction places a fundamental limitation on the distance an optical beam propagates before its size increases and spatial details blur. We show here that imposing a judicious correlation between spatial and spectral degrees of freedom of a pulsed beam can render its transverse spatial profile independent of location along the propagation axis, thereby arresting the spread of the time-averaged beam. Such correlation introduced into a beam with arbitrary spatial profile enables spatio-temporal dispersion to compensate for purely spatial dispersion that underlies diffraction. As a result, the spatio-temporal profile in the local time-frame of the pulsed beam remains invariant at all positions along the propagation axis. One-dimensional diffraction-free *space-time beams* are described – including non-accelerating Airy beams, despite the well-known fact that cosine waves and accelerating Airy beams are the only one-dimensional diffraction-free solutions to the *monochromatic* Helmholtz equation.

OCIS codes: (070.7345) Wave propagation; (050.1940) Diffraction; (260.1960) Diffraction theory; (320.5550) Pulses.

References and links

1. J. W. Goodman, *Introduction to Fourier Optics* (Roberts & Company, 2005).
2. B. E. A. Saleh and M. C. Teich, *Fundamentals of Photonics* (John Wiley & Sons, Inc., 2007).
3. A. P. Kiselev, "Localized light waves: Paraxial and exact solutions of the wave equation (a review)," Opt. Spectrosc. **102**, 603–622 (2007).
4. J. Turunen and A. T. Friberg, "Propagation-invariant optical fields," Prog. Opt. **54**, 1–88 (2010).
5. U. Levy, S. Derevyanko, and Y. Silberberg, "Light modes of free space," Prog. Opt. **61**, 237–281 (2016).
6. M. V. Berry, "Nonspreading wave packets," Am. J. Phys. **47**, 264–267 (1979).
7. G. A. Siviloglou and D. N. Christodoulides, "Accelerating finite energy Airy beams," Opt. Lett. **32**, 979–981 (2007).
8. G. A. Siviloglou, J. Broky, A. Dogariu, and D. N. Christodoulides, "Observation of accelerating Airy beams," Phys. Rev. Lett. **99**, 213901 (2007).
9. J. Durnin, "Exact solutions for nondiffracting beams. I. The scalar theory," J. Opt. Soc. Am. A **4**, 651–654 (1987).
10. J. Durnin, J. J. Miceli, and J. H. Eberly, "Diffraction-free beams," Phys. Rev. Lett. **58**, 1499–1501 (1987).
11. M. A. Bandres, J. C. Gutiérrez-Vega, and S. Chávez-Cerda, "Parabolic nondiffracting optical wave fields," Opt. Lett. **29**, 44–46 (2004).
12. B. M. Rodríguez-Lara, "Normalization of optical Weber waves and Weber-Gauss beams," J. Opt. Soc. Am. A **27**, 327–332 (2010).
13. M. A. Bandres and B. M. Rodríguez-Lara, "Nondiffracting accelerating waves: Weber waves and parabolic momentum," New J. Phys. **15**, 013054 (2013).
14. J. C. Gutierrez-Vega, R. M. Rodriguez-Dagnino, M. A. Meneses-Nava, and S. Chavez-Cerda, "Mathieu functions, a visual approach," Am. J. Phys. **71**, 233–242 (2003).
15. R. Piestun and J. Shamir, "Generalized propagation-invariant wave fields," J. Opt. Soc. Am. A **15**, 3039–3044 (1998).
16. R. Piestun, Y. Y. Schechner, and J. Shamir, "Propagation-invariant wave fields with finite energy," J. Opt. Soc. Am. A **17**, 294–303 (2000).
17. E. DelRe, F. Di Mei, J. Parravicini, G. Parravicini, A. J. Agranat, and C. Conti, "Subwavelength anti-diffracting beams propagating over more than 1,000 Rayleigh lengths," Nat. Photon. **9**, 228–232 (2015).
18. H. Sõnajalg, M. Rätsep, and P. Saari, "Demonstration of the Bessel-X pulse propagating with strong lateral and longitudinal localization in a dispersive medium," Opt. Lett. **22**, 310–312 (1997).
19. P. Di Trapani, G. Valiulis, A. Piskarskas, O. Jedrkiewicz, J. Trull, C. Conti, and S. Trillo, "Spontaneously generated X-shaped light bullets," Phys. Rev. Lett. **91**, 093904 (2003).
20. M. A. Porras and P. Di Trapani, "Localized and stationary light wave modes in dispersive media," Phys. Rev. E **69**, 066606 (2004).
21. S. Longhi, "Localized subluminal envelope pulses in dispersive media," Opt. Lett. **29**, 147–149 (2004).
22. H. E. Hernández-Figuero, M. Zamboni-Rached, and E. Recami, *Localized Waves* (John Wiley & Sons, Inc., 2008).
23. Y. Silberberg, "Collapse of optical pulses," Opt. Lett. **15**, 1282–1284 (1990).

#280396 http://dx.doi.org/10.1364/OE.24.028659
Journal © 2016 Received 2 Sep 2016; revised 17 Nov 2016; accepted 20 Nov 2016; published 2 Dec 2016

Optics EXPRESS

24. B. A. Malomed, D. Mihalache, F. Wise, and L. Torner, "Spatiotemporal optical solitons," J. Opt. B **7**, R53–R72 (2005).
25. A. Chong, W. H. Renninger, D. N. Christodoulides, and F. W. Wise, "Airy–Bessel wave packets as versatile linear light bullets," Nat. Photon. **4**, 103–106 (2010).
26. M. A. Porras, "Diffraction-free and dispersion-free pulsed beam propagation in dispersive media," Opt. Lett. **26**, 1364–1366 (2001).
27. W. Hu and H. Guo, "Ultrashort pulsed bessel beams and spatially induced group-velocity dispersion," J. Opt. Soc. Am. A **19**, 49–53 (2002).
28. R. W. Ziolkowski and J. B. Judkins, "Propagation characteristics of ultrawide-bandwidth pulsed Gaussian beams," J. Opt. Soc. Am. A **9**, 2021–2030 (1992).
29. B. J. Sussman, R. Lausten, and A. Stolow, "Focusing of light following a 4-f pulse shaper: Considerations for quantum control," Phys. Rev. A **77**, 043416 (2008).
30. F. Frei, A. Galler, and T. Feurer, "Space-time coupling in femtosecond pulse shaping and its effects on coherent control," J. Chem. Phys. **130**, 034302 (2009).
31. G. Pariente, V. Gallet, A. Borot, O. Gobert, and F. Quéré, "Space–time characterization of ultra-intense femtosecond laser beams," Nat. Photon. **10**, 547–553 (2016).
32. M. Duocastella and C. Arnold, "Bessel and annular beams for materials processing," Laser Photon. Rev. **6**, 607–621 (2012).
33. J. Baumgartl, M. Mazilu, and K. Dholakia, "Optically mediated particle clearing using Airy wavepackets," Nat. Photon. **2**, 675–678 (2008).
34. A. Dogariu, S. Sukhov, and J. Sáenz, "Optically induced 'negative forces'," Nat. Photon. **7**, 24–27 (2012).
35. T. Tanabe, H. Tanabe, Y. Teramura, and F. Kannari, "Spatiotemporal measurements based on spatial spectral interferometry for ultrashort optical pulses shaped by a Fourier pulse shaper," J. Opt. Soc. Am. B **19**, 2795–2802 (2002).
36. T. Tanab, F. Kannari, F. Korte, J. Koch, and B. Chichkov, "Influence of spatiotemporal coupling induced by an ultrashort laser pulse shaper on a focused beam profile," Appl. Opt. **44**, 1092–1098 (2005).
37. A. M. Weiner, *Ultrafast Optics* (John Wiley & Sons, Inc., 2009).
38. R. J. C. Spreeuw, "A classical analogy of entanglement," Found. Phys. **28**, 361–374 (1998).
39. A. Luis, "Coherence, polarization, and entanglement for classical light fields," Opt. Commun. **282**, 3665–3670 (2009).
40. C. V. S. Borges, M. Hor-Meyll, J. A. O. Huguenin, and A. Z. Khoury, "Bell-like inequality for the spinâĂŞorbit separability of a laser beam," Phys. Rev. A **82**, 033833 (2010).
41. A. Holleczek, A. Aiello, C. Gabriel, C. Marquardt, and G. Leuchs, "Classical and quantum properties of cylindrically polarized states of light," Opt. Express **19**, 9714–9736 (2011).
42. X.-F. Qian and J. H. Eberly, "Entanglement and classical polarization states," Opt. Lett. **36**, 4110–4112 (2011).
43. K. H. Kagalwala, G. Di Giuseppe, A. F. Abouraddy, and B. E. A. Saleh, "Bell's measure in classical optical coherence," Nat. Photon. **7**, 72–78 (2013).
44. K. H. Kagalwala, H. E. Kondakci, A. F. Abouraddy, and B. E. A. Saleh, "Optical coherency matrix tomography," Sci. Rep. **5**, 15333 (2015).
45. S. Berg-Johansen, F. Töppel, B. Stiller, P. Banzer, M. Ornigotti, E. Giacobino, G. Leuchs, A. Aiello, and C. Marquardt, "Classically entangled optical beams for high-speed kinematic sensing," Optica **2**, 864–868 (2015).
46. A. Aiello, F. Töppel, C. Marquardt, E. Giacobino, and G. Leuchs, "Quantum-like nonseparable structures in optical beams," New J. Phys. **17**, 043024 (2015).
47. F. Gori, G. Guattari, and C. Padovani, "Bessel-gauss beams," Opt. Commun. **64**, 491–495 (1987).
48. J. C. Gutiérrez-Vega and M. A. Bandres, "Helmholtz–Gauss waves," J. Opt. Soc. Am. A **22**, 289–298 (2005).
49. A. M. Weiner, J. P. Heritage, and E. M. Kirschner, "High-resolution femtosecond pulse shaping," J. Opt. Soc. Am. B **5**, 1563–1572 (1988).
50. A. M. Weiner, "Femtosecond pulse shaping using spatial light modulators," Rev. Sci. Instrum. **71**, 1929–1960 (2000).
51. C.-B. Huang, Z. Jiang, D. Leaird, J. Caraquitena, and A. Weiner, "Spectral line-by-line shaping for optical and microwave arbitrary waveform generations," Laser Photon. Rev. **2**, 227–248 (2008).
52. C. Maurer, A. Jesacher, S. Bernet, and M. Ritsch-Marte, "What spatial light modulators can do for optical microscopy," Laser Photon. Rev. **5**, 81–101 (2011).
53. D. Dan, M. Lei, B. Yao, W. Wang, M. Winterhalder, A. Zumbusch, Y. Qi, L. Xia, S. Yan, Y. Yang, P. Gao, T. Ye, and W. Zhao, "DMD-based LED-illumination super-resolution and optical sectioning microscopy," Sci. Rep. **3**, 1116 (2013).
54. A. Forbes, A. Dudley, and M. McLaren, "Creation and detection of optical modes with spatial light modulators," Adv. Opt. Photon. **8**, 200–227 (2016).
55. R. M. Koehl, T. Hattori, and K. A. Nelson, "Automated spatial and temporal shaping of femtosecond pulses," Opt. Commun. **157**, 57–61 (1998).
56. T. Feurer, J. C. Vaughan, R. M. Koehl, and K. A. Nelson, "Multidimensional control of femtosecond pulses by use of a programmable liquid-crystal matrix," Opt. Lett. **27**, 652–654 (2002).
57. J. C. Vaughan, T. Feurer, and K. A. Nelson, "Automated two-dimensional femtosecond pulse shaping," J. Opt. Soc. Am. B **19**, 2489–2495 (2002).

Optics EXPRESS

58. J. C. Vaughan, T. Feurer, and K. A. Nelson, "Automated spatiotemporal diffraction of ultrashort laser pulses," Opt. Lett. **28**, 2408–2410 (2003).
59. J. C. Vaughan, T. Hornung, T. Feurer, and K. A. Nelson, "Diffraction-based femtosecond pulse shaping with a two-dimensional spatial light modulator," Opt. Lett. **30**, 323 (2005).
60. E. Frumker and Y. Silberberg, "Femtosecond pulse shaping using a two-dimensional liquid-crystal spatial light modulator." Opt. Lett. **32**, 1384–1386 (2007).
61. E. Frumker and Y. Silberberg, "Phase and amplitude pulse shaping with two-dimensional phase-only spatial light modulators," J. Opt. Soc. Am. B **24**, 2940–2947 (2007).
62. K. J. Parker and M. A. Alonso, "The longitudinal iso-phase condition and needle pulses," Opt. Express, (in press) (2016).

1. Introduction

When a beam of light propagates freely, diffraction leads to transverse spreading and blurring of spatial details [1, 2]. Circumventing this constraint has prompted the development of 'diffraction-free' beams, which are monochromatic solutions of the Helmholtz or paraxial wave equations whose transverse spatial profiles evolve self-similarly [3–5]. In one dimension (1D), it can be demonstrated that only (accelerating) Airy Beams [6–8] and cosine waves [5] propagate self-similarly. More options are available in two dimensions (2D), including Bessel [9, 10], Weber [11–13], and Mathieu beams [14], among a hierarchy of possibilities [5, 15, 16]. Optical nonlinearities can be exploited instead to preserve the beam profile [17], but this typically requires the use of *pulsed* beams. However, maintaining the spatial profile *and* pulse shape – so-called 'light bullets' – is challenging because such waves require either a specific material dispersion [18–22] or nonlinearity, whereupon they become unstable [23,24]. It is useful to search for free-space diffraction-free solutions in light of their wide range of potential applications. Along these lines, if the spectral and spatial spatial degrees of freedom (DoFs) of the optical field are separable, each can make use of standard solutions; e.g., an Airy pulse waveform (the only known 1D solution) and a Bessel-beam spatial profile [25]. In other configurations, the pulsed beam disperses temporally even when the spatial profile is maintained [26, 27].

Here we show that an optical beam having an arbitrary transverse *spatial* profile in 1D or 2D can in principle become independent of the location along the propagation axis – given the availability of a sufficient *spectral* bandwidth. The underlying principle is the introduction of correlations between the beam's spatial and spectral DoFs by assigning each transverse wave vector component to a single wavelength according to a prescribed rule. Spatio-temporal coupling – which is typically undesirable – occurs naturally during the propagation of ultrafast pulsed beams [28–30] or the generation of ultra-high-power laser pulses [31]. Here we exploit *intentionally introduced* space-time (ST) correlations to eliminate axial variations in a pulsed beam during propagation by compensating for the spatial dispersion that underpins diffraction with spatio-temporal dispersion. We examine several examples, including diffraction-free Gaussian beams, 'bottle' beams with a non-diffracting null, and *non*-accelerating Airy beams. Such ST beams may have applications in laser manufacturing [32], 3D optical lattices, and particle trapping and manipulation [33, 34].

2. Diffraction of pulsed beams

A 1D pulsed optical beam evolves according to

$$f(x,z;t)=\iint dk_x d\omega F(k_x,\omega)e^{i\{k_x x+k_z(k_x,\omega)z-\omega t\}}; \tag{1}$$

here x and z are the transverse and axial coordinates, respectively, k_x and k_z are the corresponding wave-vector components, and the ST spectrum $F(k_x,\omega)$ is the Fourier transform of the initial field $f(x,0;t)$. For a *monochromatic beam* $\omega=\omega_o$, $F(k_x,\omega)=F(k_x)\delta(\omega-\omega_o)$ so that $f(x,z;t)=f(x,z;0)e^{-i\omega_o t}$ and diffraction is driven by spatial dispersion $k_z^2=(\omega_o/c)^2-k_x^2$. Such

Optics EXPRESS

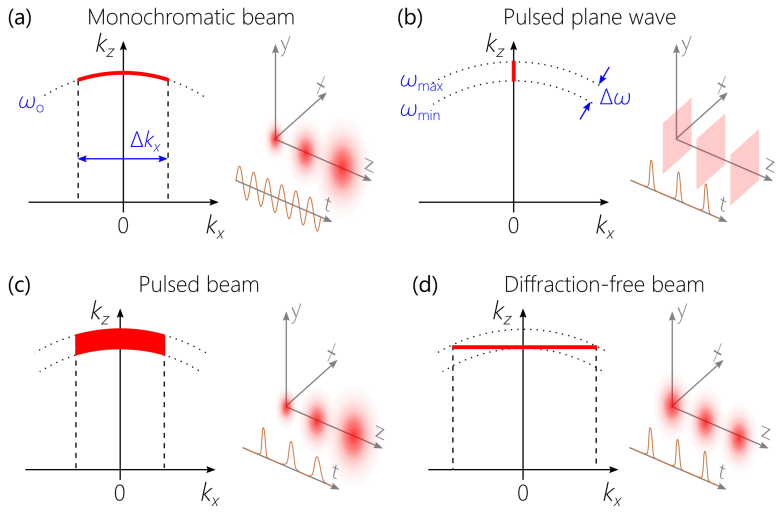

Fig. 1. Representations of optical beams in (k_x, k_z) space. Each point uniquely identifies a monochromatic plane wave $(k_x, k_z; \omega)$, $\omega = c\sqrt{k_x^2 + k_z^2}$. A circle in this plane represents all possible iso-frequency plane waves. (a) A monochromatic beam of spatial bandwidth Δk_x is represented by the red arc. This representation captures the plane waves needed in constructing such a beam but not its actual shape, which depends on the amplitudes $F(k_x)$. (b) A pulsed plane wave of spectral bandwidth $\Delta\omega$ represented by the vertical red line. (c) A pulsed beam of spatial and spectral bandwidths Δk_x and $\Delta\omega$, respectively, is represented by the red patch. The beam diffracts and the pulse waveform disperses. (d) A diffraction-free *space-time* beam represented by a *horizontal* red line corresponding to a constant $k_z = \mathcal{K}$. Both spatial and temporal profiles are z-independent.

a beam is represented in (k_x, k_z)-space by an arc of an origin-centered circle whose horizontal extent is the spatial bandwidth Δk_x [in Fig. 1(a)]. Each point in the (k_x, k_z)-plane identifies a monochromatic plane wave. Alternatively, a *pulsed plane wave* $f(x, z; t) = f(0, z; t)$ for which $F(k_x, \omega) = F(\omega)\delta(k_x)$ is represented in (k_x, k_z)-space by a vertical line whose radial extent is the bandwidth $\Delta\omega$ [Fig. 1(b)].

In general, the ST spectrum $F(k_x, \omega)$ for a pulsed beam is taken to separate into a product of spatial $F_x(k_x)$ and temporal $F_t(\omega)$ contributions [the shaded region in Fig. 1(c)], so that the initial beam in turn separates in space and time $f(x, 0; t) = f_x(x) f_t(t)$. Nevertheless, the beam subsequently loses this separability – a phenomenon known as 'space-time' coupling in the propagation and focusing of ultra-short pulses [28–30, 35–37] – as a consequence of the non-separability of k_x and ω in the integral in Eq. (1). We still have $k_x^2 + k_z^2 = (\omega/c)^2$, but the complementarity between k_x and k_z is no longer strict because ω varies over $\Delta\omega$ and each k_x can be associated with a continuum of frequencies ω and hence axial wave numbers k_z. Spatial dispersion is thus compounded with ST dispersion: the beam diffracts and the pulse disperses.

3. Diffraction-free space-time beams

We now show that an alternative exists to thwart diffraction. *Any* monochromatic plane wave (k_x, ω) may be excited when $k_x < \omega/c$ and is associated with a particular k_z. The key insight is that there exists a trajectory in (k_x, k_z) space that guarantees all the constituent plane waves have the *same* k_z: the k_z-iso-surface $k_z(k_x, \omega) = \mathcal{K}$ that fixes a hyperbolic relationship between k_x and ω,

$$\mathcal{K}^2 = (\omega/c)^2 - k_x^2. \tag{2}$$

Optics EXPRESS

Such a pulsed beam is represented in (k_x, k_z)-space by a horizontal line [Fig. 1(d)]. This one-to-one correspondence between $|k_x|$ and ω – by imposing the constraint $\omega(k_x) = \omega_x$ on the (k_x, ω) pairings – entails that each spatial frequency k_x is 'encoded' on a single frequency ω to ensure that k_z is independent of both k_x and ω. Such a beam evolves self-similarly except for an overall phase,

$$f(x, z; t) = e^{i\mathcal{K}z} \int dk_x F(k_x) e^{i(k_x x - \omega_x t)} = e^{i\mathcal{K}z} g(x; t). \tag{3}$$

Crucially, in this conception we need not restrict ourselves to any *specific* 1D beam profile to achieve diffraction-free propagation. The only requirement is to use a sufficient bandwidth $\Delta\omega$ of the auxiliary spectral DoF to 'protect' the beam's spatial DoF [Fig. 1(d)],

$$\Delta\omega = \omega_{\max} - \omega_{\min} = (c\Delta k_x)^2 / 2\omega_o, \tag{4}$$

where $\omega_{\min} = c\mathcal{K}$, $\omega_{\max}^2 = \omega_{\min}^2 + (c\Delta k_x)^2$, and $\omega_o = (\omega_{\max} + \omega_{\min})/2$. This bandwidth is necessary to 'protect' the beam and arrest its spreading. In general, a *broader* spectrum is required to protect a beam with larger Δk_x (i.e., *finer* details). Therefore, a beam with a highly localized transverse profile becomes associated with a highly localized pulse; that is, there is a correlation between localization in space and time in this conception. We refer to such a beam as a 'space-time' (ST) beam since the two DoFs are inextricably intertwined or 'entangled'. The notion of 'classical entanglement' has recently attracted considerable attention [38–46]. Most previous experimental and theoretical studies of classical entanglement have focused on optical beams in which correlations exist between discretized DoFs, such as polarization or a few spatial modes. The diffraction-free ST beams described here rely instead on correlation between two continuous DoFs (ω and k_x).

The generalization to 2D optical beams is straightforward. We assign to each transverse spatial frequency $\mathbf{k}_T = (k_x, k_y)$ in the 2D spatial spectrum $F_x(k_x, k_y)$ the frequency ω such that $k_z = \sqrt{|\mathbf{k}_T|^2 - (\omega/c)^2} = \mathcal{K}$, which guarantees diffraction-free propagation. Therefore, all 2D transverse spatial frequencies such that $k_x^2 + k_y^2 =$ constant are encoded on the same frequency ω.

4. Examples of diffraction-free ST beams

To illustrate the concept of a diffraction-free ST beam, we present in Fig. 2 an example of a Gaussian beam in two configurations. The traditional case of a Gaussian beam of FWHM $x_o = 10$ μm and spectral bandwidth of $\Delta\lambda = 0.01$ nm (corresponding to a FWHM pulse-width of 94 ps) is shown in Fig. 2(a)-2(d). The ST spectrum $F(k_x; \lambda) = F_x(k_x) F_t(\lambda)$ is *separable* [Fig. 2(a)] and so is the initial ST intensity $|f(x, 0; t)|^2$ [Fig. 2(b)]. The beam profile diffracts with a Rayleigh range of $z_R = \pi w_o^2/\lambda \approx 283$ μm (w_o is the Gaussian beam radius [2]) [Fig. 2(c)], whether at the pulse center $|f(x, z; 0)|^2$ or in the time-averaged profile $\int dt |f(x, z; t)|^2$. The contribution of the beam center to the pulse $|f(0, z; t)|^2$ consequently drops [Fig. 2(d)], while the spatially averaged pulse $\int dx |f(x, z; t)|^2$ is axi-symmetric [Fig. 2(d), inset]. Increasing the bandwidth here reduces the pulse-width and increases the ST coupling effects [2].

By introducing hyperbolic ST spectral correlations according to Eq. (2), we obtain the non-separable spectrum in Fig. 2(e) from Fig. 2(a). Each k_x is correlated to a specific λ with an *uncertainty* of $\delta\lambda$, whereas the bandwidth $\Delta\lambda$ is determined by Δk_x (Eq. (4)). The beam size $x_o = 10$ μm requires an associated bandwidth of ≈ 1 nm. The ST intensity is no longer separable and is instead localized around $x = 0$ and $t = 0$ for *all* z. The transverse sections of the beam $|f(x, z; 0)|^2$ and $\int dt |f(x, z; t)|^2$ are invariant upon propagating a distance $20 z_R$ [Fig. 2(g)], whereupon the Gaussian beam of identical spatial bandwidth has increased 20-fold in width [Fig. 2(c)]. Note that the pulsewidth at $x = 0$ is determined by $\Delta\lambda$ [Fig. 2(h)] whereas the spatially averaged pulsewidth is set by $\delta\lambda$ [Fig. 2(h), inset]. Note also that a delay in the pulse at $x = 0$ emerges as a result of the reorganization of energy in the time-frame of the pulse after

Optics EXPRESS

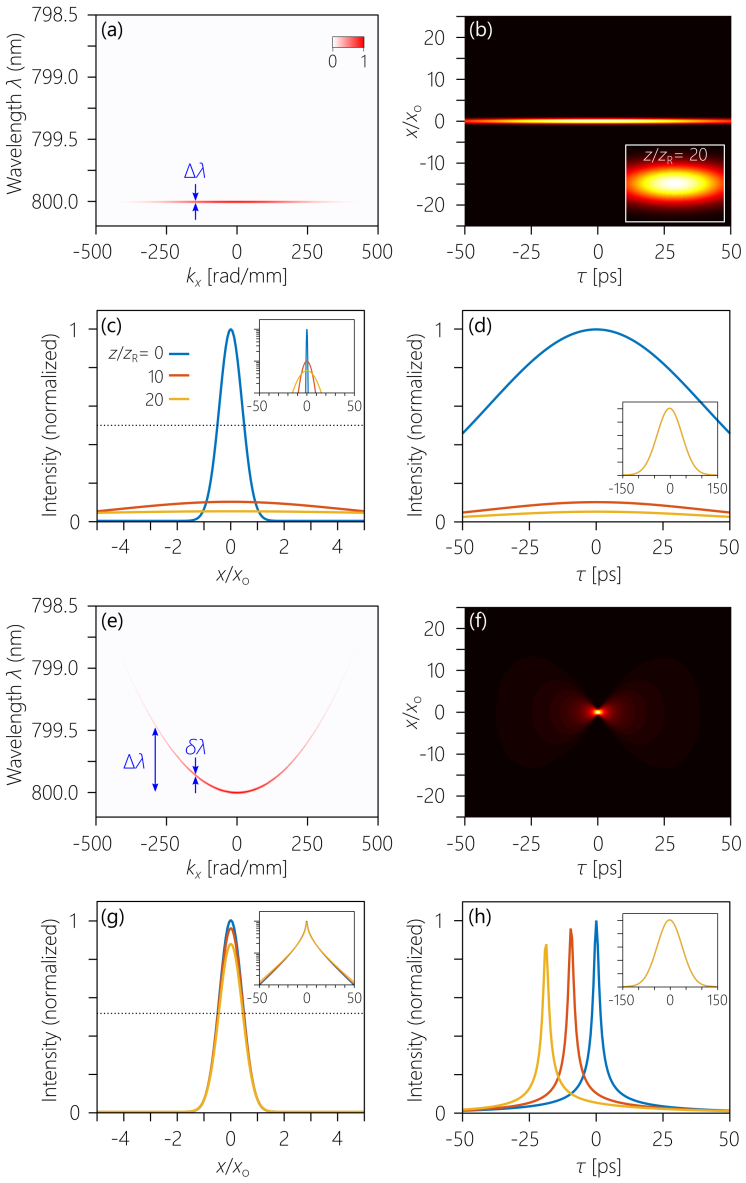

Fig. 2. (a) ST spectrum $F(k_x, \lambda)$ for a Gaussian beam of initial FWHM $x_o = 10$ μm and $\Delta\lambda = 0.01$ nm. (b) ST intensity $|f(x, 0; t)|^2$ at $z = 0$. Inset shows $|f(x, z; t)|^2$ at $z/z_R = 20$. (c) Beam profile $|f(x, z; 0)|^2$ at $z/z_R = 0, 10, 20$. The beam profiles correspond to the peaks of the pulses at each z. Inset shows the time-averaged profile $\int dt |f(x, z; t)|^2$ at the same z. (d) Pulse shape $|f(0, z; t)|^2$ at the beam center for $z/z_R = 0, 10, 20$. Inset is the spatially averaged pulse shape $\int dx |f(x, z; t)|^2$, which is independent of z. All color maps are normalized independently. (e)-(h) Correspond to (a)-(d) except that ST correlations are introduced between k_x and λ; $\delta\lambda = 0.01$ nm and $\Delta\lambda = 1$ nm. (e) The ST spectrum $F(k_x, \lambda)$. (f) The ST intensity $|f(x, 0; t)|^2$ is localized in x and t. The inset is removed since there is no axial variation. (g) Beam profile $|f(x, z; 0)|^2$ at $z/z_R = 0, 10, 20$. The beam profile is z-invariant. (h) Pulse shape $|f(0, z; t)|^2$ at the beam center for $z/z_R = 0, 10, 20$. Inset is the spatially averaged pulse shape $\int dx |f(x, z; t)|^2$, which is independent of z.

Optics EXPRESS

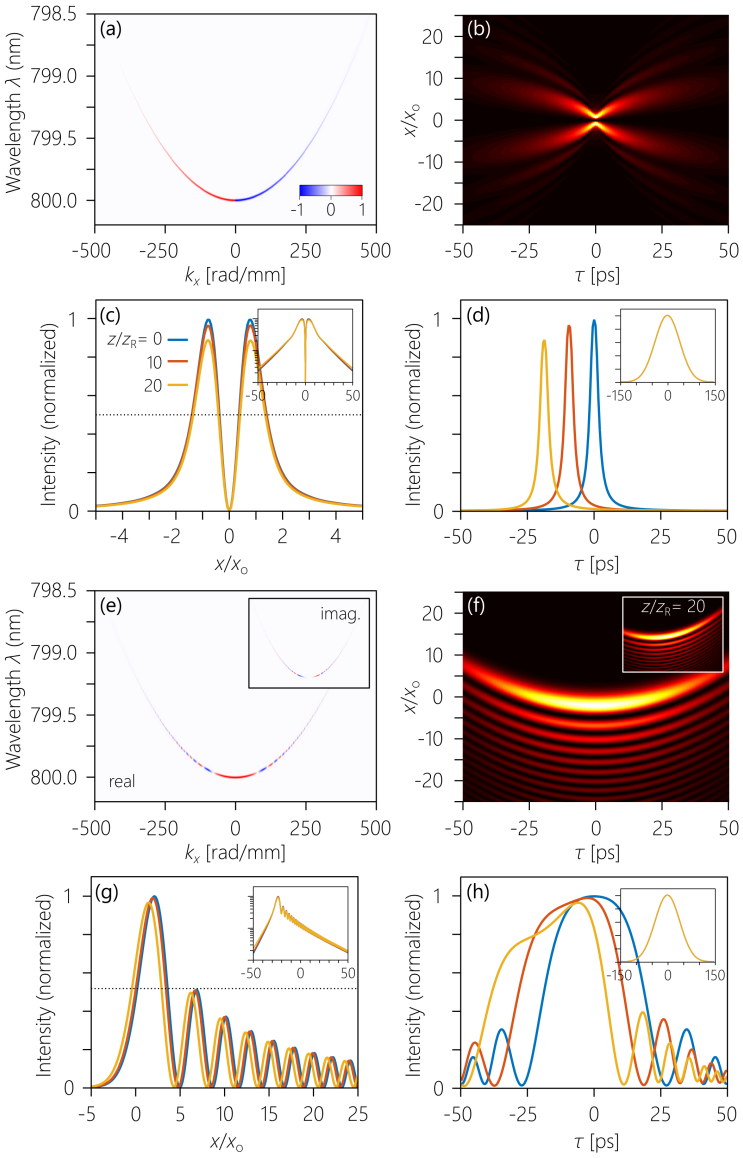

Fig. 3. Diffraction-free beams of arbitrary spatial profile with ST correlations introduced between k_x and λ; the correlation uncertainty is $\delta\lambda$ = 0.01 nm and the bandwidth is $\Delta\lambda = 1$ nm. (a) ST spectrum $F(k_x, \lambda)$ for a 'bottle-beam,' where the phase along the spatio-temporal spectrum is phase-modulated to create an odd-parity beam with a minimum at its center. (b) ST intensity $|f(x, 0; t)|^2$ at $z = 0$. The inset is removed since there is no axial variation. (c) Beam profile $|f(x, z; 0)|^2$ at $z/z_R = 0, 10, 20$. The beam profiles correspond to the peaks of the pulses at each z. Inset shows the time-averaged profile $\int dt |f(x, z; t)|^2$ at the same z. (d) Pulse shape $|f(0, z; t)|^2$ at the beam center for $z/z_R = 0, 10, 20$. Inset is the spatially averaged pulse shape $\int dx |f(x, z; t)|^2$, which is independent of z. All color maps are normalized independently. (e)-(h) Correspond to (a)-(d) except that the phase modulation is $e^{-i\pi(k_x x_o)^3}$, which is designed to produce a *non*-accelerating Airy beam. (e) Real part of the ST spectrum $F(k_x, \lambda)$, while the inset shows the imaginary part. (f) ST intensity $|f(x, 0; t)|^2$ at $z = 0$. (g) Beam profile $|f(x, z; 0)|^2$ at $z/z_R = 0, 10, 20$. Inset shows the time-averaged profile $\int dt |f(x, z; t)|^2$ at the same z. (h) Pulse shape $|f(0, z; t)|^2$ at the beam center for $z/z_R = 0, 10, 20$. Inset is the spatially averaged pulse shape $\int dx |f(x, z; t)|^2$, which is independent of z.

Optics EXPRESS

propagating for a long distance [Fig. 2(h)], whereupon different parts of the transverse wave front shift in time with respect to the center of the time-frame (we only plot the pulse at $x=0$). Once the beam is integrated over the transverse plane, these local time delays vanish [Fig. 2(h), inset]. Here, we also note that the smaller transverse width of the ST beam desired, the bigger bandwidth $\Delta\lambda$ is required, resulting in a narrower pulsewidth at $x=0$.

A unique advantage of our approach is that diffraction-free propagation is ensured by satisfying the constraint in Eq. (2) without reference to the actual ST spectrum. Consequently, by modulating $F(k_x, \lambda)$ we produce diffraction-free pulsed beams of arbitrary profiles. We present two examples in Fig. 3. In the first [Fig. 3(a)-3(d)], we modulate the spectrum in Fig. 2(a) with a phase term of the form $e^{i\pi u(k_x)}$, where $u(\cdot)$ is the unit-step function, so the spectrum is odd along k_x. The corresponding axially self-similar ST intensity [Fig. 3(b)] now has a null at $x=0$: $|f(0,z;t)|^2=0$ and $\int dt|f(0,z;t)|^2=0$. The result is a 'bottle-beam' with a diffraction-free null along z. A second example is provided in Fig. 3(e)-3(h) where the spectrum is modulated by the phase $e^{-i\pi(k_x x_o)^3}$, which produces a diffraction-free Airy profile [Fig. 3(g)]. Note, crucially, that the Airy profile here is not accelerating transversely and is thus a truly diffraction-free beam, in contrast to accelerating monochromatic Airy beams.

5. Impact of uncertainty on diffraction-free length

The diffraction-free length is determined by the uncertainty in the relationship $\omega(k_x)=\omega_x$, which is subject to practical restrictions on ST beam generation. In Fig. 4, we further relax the

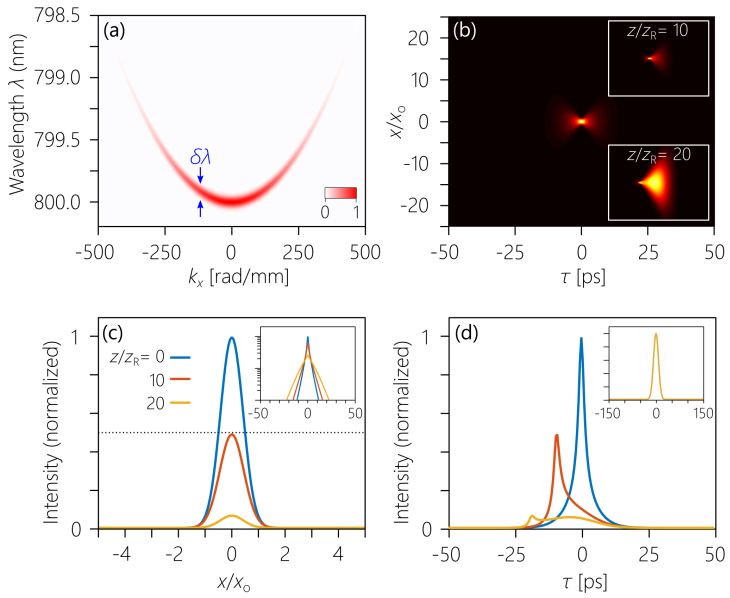

Fig. 4. The impact of the ST correlation uncertainty $\delta\lambda$ on the diffraction-free propagation length. (a) ST spectrum $F(k_x, \lambda)$ for a Gaussian beam with ST correlations introduced between k_x and λ; $\delta\lambda = 0.05$ nm and $\Delta\lambda = 1$ nm. (b) ST intensity $|f(x,0;t)|^2$ at $z=0$. Insets show $|f(x,z;t)|^2$ at $z/z_R = 10, 20$. (c) Beam profile $|f(x,z;0)|^2$ at $z/z_R = 0, 10, 20$. The beam profiles correspond to the peaks of the pulses at each z. Inset shows the time-averaged profile $\int dt|f(x,z;t)|^2$ at the same z. (d) Pulse shape $|f(0,z;t)|^2$ at the beam center for $z/z_R = 0, 10, 20$. Inset is the spatially averaged pulse shape $\int dx|f(x,z;t)|^2$, which is independent of z. The pulse at the beam center $|f(0,z;t)|^2$ undergoes z-dependent delay and deformation. All color maps are normalized independently.

Optics EXPRESS

ST correlations and increase $\delta\lambda$ to 0.05 nm and find that the initial ST intensity $|f(x,0;t)|^2$ now diffracts [Fig. 4(c)] over the same axial range considered in Fig. 2 and Fig. 3, where the reduced correlation uncertainty ($\delta\lambda = 0.01$ nm) arrests the beam spread.

We have examined thus far ST beams propagating across distances over which traditional beams of comparable spatial bandwidth diffract significantly ($\sim 20 z_R$). Because of the finite correlation uncertainty $\delta\lambda$, it is critical to examine the propagation of the beam at larger z. The width of a Gaussian beam increases linearly when $z \gg z_R$ at a rate inversely proportional to the initial width [2]. Considering a ST beam having the same spatial bandwidth and a correlation uncertainty of $\delta\lambda = 0.05$ nm, we find the diffraction dynamics delineated into two regimes: a slow diffraction regime for $z < 3$ mm followed by a fast diffraction regime in which the width approaches that of the traditional Gaussian beam [47,48]. Here, we define critical distance z_c that occurs at the knee separating 'slow' and 'fast' diffraction regimes (Fig. 5). Decreasing the uncertainty to $\delta\lambda = 0.01$ nm increases z_c to ≈ 16 mm [Fig. 5].

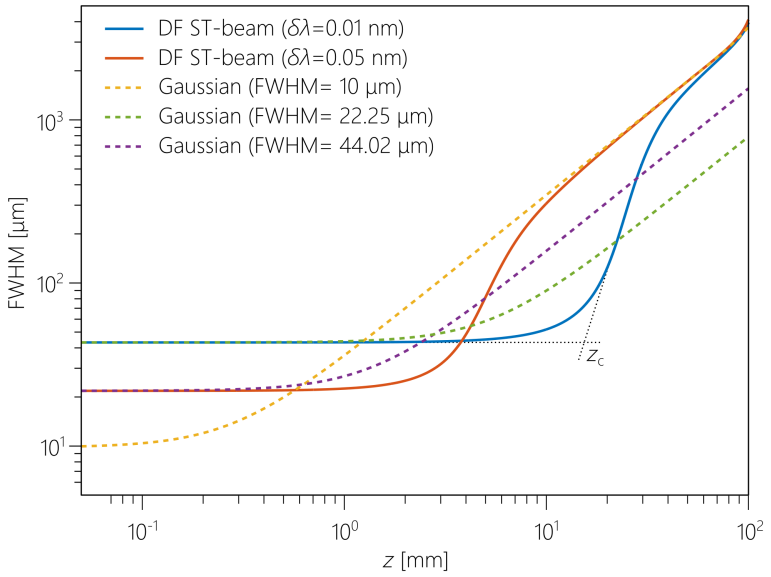

Fig. 5. Impact of ST correlation uncertainty on the diffraction-free (DF) range z_c of ST beams compared to monochromatic Gaussian beams ($\Delta\lambda = 0.01$ nm). Smaller $\delta\lambda$ increases z_c.

6. Proposed realization for diffraction-free ST beams

The question remains of the feasibility of constructing such diffraction-free ST beams. We propose an arrangement that combines traditional approaches of pulse-shaping [49–51] with those for beam-shaping [52–54]. Starting with a separable pulsed beam $f(x,t) = f_x(x) f_t(t)$, where the beam profile $f_x(x)$ is generic (e.g., the TEM_{00} mode of a pulsed laser), the pulse spectrum is dispersed along the y-direction via a diffraction grating and then directed to a 2D spatial light modulator (SLM) that imprints a phase distribution in the transverse x–y plane of the form $e^{ik_x(y)x}$ (see [55–61]). Since the spectrum is spread along y, each spatial frequency $k_x(y)$ is selected to correlate correctly to the wavelength at position y according to Eq. (2). A second diffraction grating combines the spectrum to reconstitute the pulse, thereby producing the desired ST beam. Preparing a diffraction-free ST beam of width 10 μm at a wavelength of 800 nm requires a 1-nm-wide spectrum and a spatial spectrum $\Delta k_x = 556$ rad/nm. These

Optics EXPRESS

requirements can be fulfilled by spreading the pulse by a diffraction grating with 1800 lines/mm that is illuminated over a 45-mm-wide section, and then directing the spectrum via a cylindrical lens of 200-mm focal length to an SLM with 5-μm-wide pixels. This system can produce the desired ST correlation with an uncertainty of $\delta\lambda = 0.01$ nm, corresponding to a diffraction length of 16 mm $\approx 55 z_{\mathrm{R}}$ of a monochromatic beam having the same spatial bandwidth Δk_x.

7. Conclusion

In conclusion, we have described a general approach to preparing diffraction-free ST beams in 1D and 2D with arbitrary cross sections. This is particularly surprising in 1D where it has been conclusively demonstrated that *only* two spatial profiles (Airy and cosine) propagate with no transverse changes – assuming monochromatic light. Relaxing the monochromaticity constraint enables ST correlations to arrest changes in the transverse beam profile along the propagation axis. Current technology can readily achieve a ST correlation-uncertainty of $\delta\lambda \approx 0.01$ nm over a bandwidth of 1 nm, which can maintain a pulsed beam of width 10 μm and pulse-width 94.1 ps over a distance of 16-mm – sufficient for deep-tissue imaging, for instance. The ST-beam concept can be applied to other manifestations of waves, such as acoustic and electron beams, for instance. Finally, the theory outlined here was formulated for coherent light in free space. It remains an open question whether this strategy can be extended to partially coherent light, to propagation in dispersive media, and propagation in the presence of scattering perturbations.

We have recently learned that another group has been studying similar pulsed beams and that their work will appear published concurrently with ours [62].

Funding

U.S. Office of Naval Research (ONR) contract N00014-14-1-0260.

Acknowledgments

We thank D. N. Christodoulides and T. M. Yarnall for helpful discussions.